NEOPLASIA
www.neoplasia.com
Volume 11 Number 11 November 2009 pp. 1155–1164 

# The Effects of Vandetanib on Paclitaxel Tumor Distribution and Antitumor Activity in a Xenograft Model of Human Ovarian Carcinoma[1,2]

**Marta Cesca*, Roberta Frapolli†, Alexander Berndt‡, Valentina Scarlato*, Petra Richter‡, Hartwig Kosmehl§, Maurizio D'Incalci†, Anderson J. Ryan¶ and Raffaella Giavazzi***

*Laboratory of Biology and Treatment of Metastases, Department of Oncology, Mario Negri Institute for Pharmacological Research, Milan, Italy; †Laboratory of Cancer Pharmacology, Department of Oncology, Mario Negri Institute for Pharmacological Research, Milan, Italy; ‡Institute of Pathology, University Hospital, Jena, Germany; §Institute of Pathology, HELIOS-Klinikum, Erfurt, Germany; ¶AstraZeneca, Alderley Park, Macclesfield, UK

## Abstract

This study was designed to determine the effects of vandetanib, a small-molecule receptor tyrosine kinase inhibitor of vascular endothelial growth factor and epidermal growth factor receptor, on paclitaxel (PTX) tumor distribution and antitumor activity in xenograft models of human ovarian carcinoma. Nude mice bearing A2780-1A9 xenografts received daily (5, 10, or 15 days) doses of vandetanib (50 mg/kg per os), combined with PTX (20 mg/kg intravenously). Morphologic and functional modifications associated with the tumor vasculature (CD31 and α-smooth muscle actin staining and Hoechst 33342 perfusion) and PTX concentrations in plasma and tumor tissues were analyzed. Activity was evaluated as inhibition of tumor growth subcutaneously and spreading into the peritoneal cavity. Vandetanib treatment produced no significant change in tumor vessel density, although a reduced number of large vessels, an increased percentage of mature vessels, and diminished tumor perfusion were evident. Pretreatment with vandetanib led to decreased tumor PTX levels within 1 hour of PTX injection, although 24 hours later, tumor PTX levels were comparable with controls. In efficacy studies, the combination of vandetanib plus PTX improved antitumor activity compared with vandetanib or PTX alone, with greater effects being obtained when PTX was administered before vandetanib. The combination of PTX plus vandetanib reduced tumor burden in the peritoneal cavity of mice and significantly increased their survival. Analysis of vascular changes and PTX tumor uptake in vandetanib-treated tumors may help to guide the scheduling of vandetanib plus PTX combinations and may have implications for the design of clinical trials with these drugs.

*Neoplasia (2009) 11, 1155–1164*

## Introduction

Angiogenesis plays a critical role in sustaining the growth of solid tumors and in promoting tumor metastasis [1,2]. Furthermore, the tumor vasculature may also influence the delivery and effectiveness of anticancer therapy [3,4]. Drugs targeting the tumor vasculature have been developed and have shown efficacy in preclinical models and, more recently, in clinical studies in several solid tumor types [2,5,6].

In general, antiangiogenic agents have provided only modest benefit as monotherapy, and therefore, they have been evaluated extensively in combination with conventional chemotherapies [7,8]. For

Address all correspondence to: Dr. Raffaella Giavazzi, Department of Oncology, Mario Negri Institute for Pharmacological Research, Via La Masa, 19, 20156 Milan, Italy.
E-mail: raffaella.giavazzi@marionegri.it

[1]This work was supported by an unrestricted research agreement with AstraZeneca (Alderley Park, Macclesfield, Cheshire, UK), the 7th EU Framework Program for Research and Technological Development (FP7) ADAMANT HEALTH-F2-2008-201342, the Italian Association for Cancer Research, and Fondazione CARIPLO (no. 2008-2264).
[2]This article refers to supplementary material, and is available online at www.neoplasia.com.
Received 28 May 2009; Revised 30 July 2009; Accepted 31 July 2009


DOI 10.1593/neo.09866

example, bevacizumab, a monoclonal antibody directed against vascular endothelial growth factor (VEGF), is currently approved for treatment of metastatic colorectal cancer, non–small cell lung cancer (NSCLC) and breast cancer, in combination with standard-of-care chemotherapy [9,10]. However, the mechanism by which antiangiogenic agents increase the efficacy of chemotherapy is not well understood.

In many cases, combination schedules are chosen empirically. To optimize the combination approaches used in the clinic, a more rational approach to combination selection may be needed, which takes into account the mechanistic and pharmacokinetic interactions of the drugs as well as the biologic modification of the tumor microenvironment [11].

Combination therapy with an antiangiogenic agent plus chemotherapy acts at multiple targets within the tumor, depriving it of nutrients and oxygen (i.e., antivascular and antiangiogenic effects) and killing highly proliferative tumor cells (i.e., cytotoxic effect) [12]. This might seem paradoxical because by modifying the tumor vasculature, antiangiogenic therapy could potentially impair the delivery of cytotoxic drugs [13].

However, the tumor vasculature is characterized by increased vessel permeability, dilatation, and tortuosity, decreased pericyte coverage, and abnormal basement membranes due to an imbalance between proangiogenic and antiangiogenic factors [14–16]. As a consequence, tumor blood flow is impaired, and this, together with compression of the blood vessels by cancers cells, can result in high interstitial fluid pressure, hypoxic regions within the tumor, and ultimately impaired drug delivery [17,18]. Recently, Jain [19] hypothesized that during antiangiogenic therapy (in particular, anti-VEGF therapy), a temporally defined "window" exists during which abnormal tumor blood vessels become morphologically "normalized," theoretically leading to improved blood flow and increased delivery of chemotherapy and oxygen to the tumor.

Changes in the tumor microenvironment, such as decreased microvessel density and vessel area, increased pericyte coverage, decreased interstitial fluid pressure, and hypoxia, after anti-VEGF therapy have been demonstrated by several investigators [20–23]. However, whether these morphologic changes are accompanied by functional modifications, such as improved drug and oxygen delivery, remains controversial [24,25]. Moreover, it has not been clearly demonstrated how an improvement in drug penetration translates into an increase in therapeutic response [22,23]. The presence of a "normalization" window may necessitate finely tuned scheduling and sequencing of antiangiogenic and cytotoxic combination therapies, although this would present significant practical challenges in the clinical setting.

Several receptor tyrosine kinase inhibitors (RTKIs) that target VEGF receptors (VEGFRs) as well as other growth factor receptor signaling pathways relevant in tumor progression are under development [7,26,27]. These agents not only directly affect tumor vasculature but also have supplemental activity on other compartments of the tumor stroma and on tumor cells themselves. Improved antitumor efficacy has been reported after their addition to chemotherapy in experimental tumor models [2,7,11,28]. Vandetanib (Zactima; AstraZeneca, Macclesfield, UK) is an orally available, small-molecule inhibitor of VEGFR-2, epidermal growth factor receptor (EGFR), and rearranged during transfection tyrosine kinases [29,30]. Effects on tumor vasculature have been described in preclinical studies with vandetanib, including reduced vascular density [30,31], decreased endothelial cell proliferation associated with apoptosis [32,33], and decreased vascular permeability [31]. In preclinical tumor models, vandetanib has shown activity as a single agent [29,30,32,33] and enhanced the activity of chemotherapy and radiotherapy [34–37].

Vandetanib is being investigated in phase 3 clinical trials in second-line NSCLC and in phase 2 trials in various tumor types including metastatic hereditary medullary thyroid cancer [38]. Recently, a randomized phase 2 study of vandetanib plus paclitaxel (PTX) and carboplatin as first-line treatment of advanced NSCLC demonstrated prolongation of progression-free survival with this triple regimen compared with PTX plus carboplatin [39]. PTX alone or in combination with carboplatin is currently used as a standard treatment in ovarian carcinoma [40].

On this ground, we decided to investigate the influence of vandetanib on the antitumor activity of PTX in a preclinical model of ovarian carcinomas. For this purpose, A2780-1A9 human ovarian carcinoma xenografts, previously characterized for angiogenic phenotype and response to PTX alone and in combination with angiogenesis inhibitors, have been used [41–43]. Modifications in the tumor vasculature and in tumor uptake of PTX after vandetanib treatment were investigated, and the results were used to rationalize the combination regimen.

## Materials and Methods

### *Drug Preparations*

Vandetanib (AstraZeneca) was suspended in 1% Tween-80 (Sigma, Milan, Italy) by gentle shaking with 4-mm glass beads at room temperature overnight, and the suspension used within 1 week of preparation. Vandetanib was administered by daily oral gavage at a dose of 50 mg/kg. Paclitaxel (PTX; kindly provided by Indena S.p.A., Milan, Italy) was dissolved in 50% Cremophor EL (Sigma) and 50% ethanol and further diluted with saline immediately before use. PTX was administered intravenously (i.v.) at a dose of 20 mg/kg. Control mice received the corresponding vehicle.

### *Animals and Xenograft Tumor Model*

Six- to eight-week-old female NCr-*nu/nu* mice were obtained from Harlan (Correzzana, Italy). Mice were maintained under specific pathogen-free conditions, housed in isolated vented cages, and handled using aseptic procedures. Procedures involving animals and their care were conducted in conformity with institutional guidelines that are in compliance with national (Legislative Decree 116 of January 27, 1992, Authorization n.169/94-A issued December 19, 1994, by Ministry of Health) and international laws and policies (EEC Council Directive 86/609, OJ L 358. 1, December 12, 1987; Standards for the Care and Use of Laboratory Animals, United States National Research Council, Statement of Compliance A5023-01, November 6, 1998). A2780-1A9 human ovarian carcinoma cells ($10 \times 10^6$) were implanted subcutaneously in the flank or into the peritoneal cavity of nude mice.

### *Vessel Analysis after Vandetanib Treatment*

A2780-1A9 tumor-bearing mice ($n = 5$; tumor weight approximately 150 mg) were treated with vandetanib or its vehicle for 5 to 15 days. One minute before killing, mice were perfused with 40 mg/kg i.v. Hoechst 33342 (Sigma). Tumors were excised and divided into two parts: one half was embedded in optimal cutting compound, snap-frozen, and stored at –80°C for immunohistochemical analyses of CD31 (vessel density and morphology), α-smooth muscle actin (α-SMA; vessel maturation), and vessel perfusion; the

other half was immediately frozen at −80°C for HPLC analysis of Hoechst 33342. Tumor tissues were processed as described in Supplementary Information 1.

### *Pharmacokinetic Analysis*

A2780-1A9 tumor-bearing mice ($n$ = 4; tumor weight approximately 150 mg) were pretreated with vandetanib or its vehicle for 5, 10, or 15 days as detailed in the Results section. Four hours after the last vandetanib (or its vehicle) dose, PTX was administered. Tumor and plasma samples were collected at different time points (15 and 30 minutes and 1, 3, 6, and 24 hours) after PTX treatment. At the indicated sampling time, mice were anesthetized, blood was collected from retro-orbital plexus into heparinized tubes, and the plasma fraction was separated. Mice were killed by cervical dislocation, and tumors excised and snap frozen. Analysis of the samples was performed by HPLC with UV detection at 230 nm as described in Supplementary Information 2. Noncompartmental pharmacokinetic parameters were estimated by WinNonlin Pro Node 4.1 pharmacokinetic software (Pharsight Co. Mountain View, CA).

### *Assessment of Antitumor Response to Vandetanib and PTX*

Mice bearing A2780-1A9 were treated with vandetanib, PTX, vandetanib plus PTX, or vehicle according to two experimental protocols. In the first protocol (Figure 5), mice were pretreated with vandetanib for 1, 5, or 10 days and randomized to received a single dose of PTX at approximately 150 mg of tumor weight; for the 5-day schedule of vandetanib, a parallel group of mice was also established to receive vandetanib after PTX. In the second protocol (Figure 6), treatment schedules (5 days vandetanib/1 dose of PTX) were repeated for three cycles, with a 5-day break between cycles. The combination of vandetanib plus PTX was administered as two different sequences of PTX administration: PTX administered 4 hours after the fifth dose of vandetanib (vandetanib → PTX) or 24 hours before the first dose of vandetanib (PTX → vandetanib).

For the subcutaneous model (8-10 mice per group), tumor growth was measured with a vernier caliper, and the estimates of tumor weights (mg = $mm^3$) calculated as follows: (length [mm] × width $[mm]^2$) / 2. Efficacy of the treatment was expressed as best tumor growth inhibition [$\%T/C$ = (median tumor weight of treated tumors/median tumor weight of control tumors) × 100] or tumor growth delay ($T - C$ = median time to reach 800 mg of treated tumor − median time to reach 800 mg of control tumor). Experiments were concluded when tumors reached a median weight of 2 ± 0.5 g.

For the intraperitoneal model (orthotopic growth), 15 mice per group were treated. At the end of the treatment period, five mice per group were killed and necropsied to establish the tumor burden. The remaining mice were monitored for tumor formation in the peritoneal cavity (abdominal distension) and killed when they became moribund (the day of death being considered the limit of survival). At autopsy, the peritoneal cavity was macroscopically examined to ascertain the presence of tumor. Results are plotted as the percentage survival against days after tumor transplant. The increment of life span (ILS) was calculated as 100 × [(median survival day of treated group − median survival day of control group) / median survival day of control group].

### *Statistical Analyses*

Statistical analyses were carried out using Prism Software (Prism 5.01; GraphPad Software, La Jolla, CA). Statistical differences for pharmacodynamic, pharmacokinetic, and therapy experiments were evaluated by two-way ANOVA followed by Bonferroni posttest; for the H33342 HPLC analyses, Student's $t$ test was used. Differences in survival were analyzed by the log-rank test. $P < .05$ was considered significant.

## Results

### *Effects of Vandetanib on Tumor Vasculature*

Tumor microvessel density, dimension and maturation were measured after the administration of vandetanib (50 mg/kg per day or vehicle control) for 5, 10, or 15 days to mice bearing A2780-1A9 tumor xenografts. As shown in Figure 1*A*, no significant difference in tumor vessel density was detected (by CD31 staining) between the vandetanib-treated group and the time-matched untreated control group after 5, 10, or 15 days of continuous treatment. However, mice treated with vandetanib had a reduction in tumor vessel dimensions (vessel area and diameter) compared with the control animals, which was evident after 10 and 15 days of vandetanib treatment (Figures 1, *B* and *C*, and 2*A*). In the control group, vessel area and diameter increased over time, whereas in the tumors from the vandetanib-treated group, vessel area and diameter remained stable or decreased slightly. A consistent decrease in large vessels percentage (vessel area > 1000 $\mu m^2$), rather than normal-sized vessels, was observed in the tumors of vandetanib-treated animals at each time point (data not shown). In contrast, we observed an increased vessel maturation index, that is, pericyte coverage, which was statistically significant after 5 days of vandetanib pretreatment (Figures 1*D* and 2*B*).

### *Distribution of PTX in Tumor Xenografts Pretreated with Vandetanib*

To assess whether vandetanib pretreatment, and the associated vascular changes, influenced tumor concentration of PTX, we studied PTX distribution in A2780-1A9 tumor xenografts of animals that had been pretreated with vandetanib (or its vehicle) for different periods and schedules (Figure 3).

In the first experiment, A2780-1A9 tumor-bearing mice were pretreated with vandetanib (or its vehicle) for 5 days (50 mg/kg per day). Four hours after the last vandetanib dose, PTX (20 mg/kg) was administered i.v., tumor and plasma samples were collected at 15 and 30 minutes and at 1, 3, 6 and 24 hours later, and PTX concentrations in the samples were evaluated by HPLC.

As shown in Figure 3*A*, PTX distribution into the tumor tissue was, in general, higher in the control group compared with in that the vandetanib-pretreated groups, with the difference in mean PTX tumor concentration between the groups reaching statistical significance at 30 minutes and at 1 and 6 hours after PTX injection.

The tumor penetration of PTX in mice pretreated with vandetanib was found to be slower than in the control mice as illustrated by the $C_{max}$ and $T_{max}$ values (Table 1). Twenty-four hours after PTX administration, tumor PTX levels were not statistically different between the two groups. PTX concentrations in plasma were comparable between the two groups (Table 1).

To study the influence of the timing of vandetanib pretreatment on PTX tumor uptake, in a second experiment, A2780-1A9 tumor-bearing mice were pretreated with vandetanib for different periods (1, 5, 10, and 15 days). Four hours after the last vandetanib dose, PTX was administered, and its concentration was determined in tumors and plasma 1 and 24 hours after its injection. As shown in

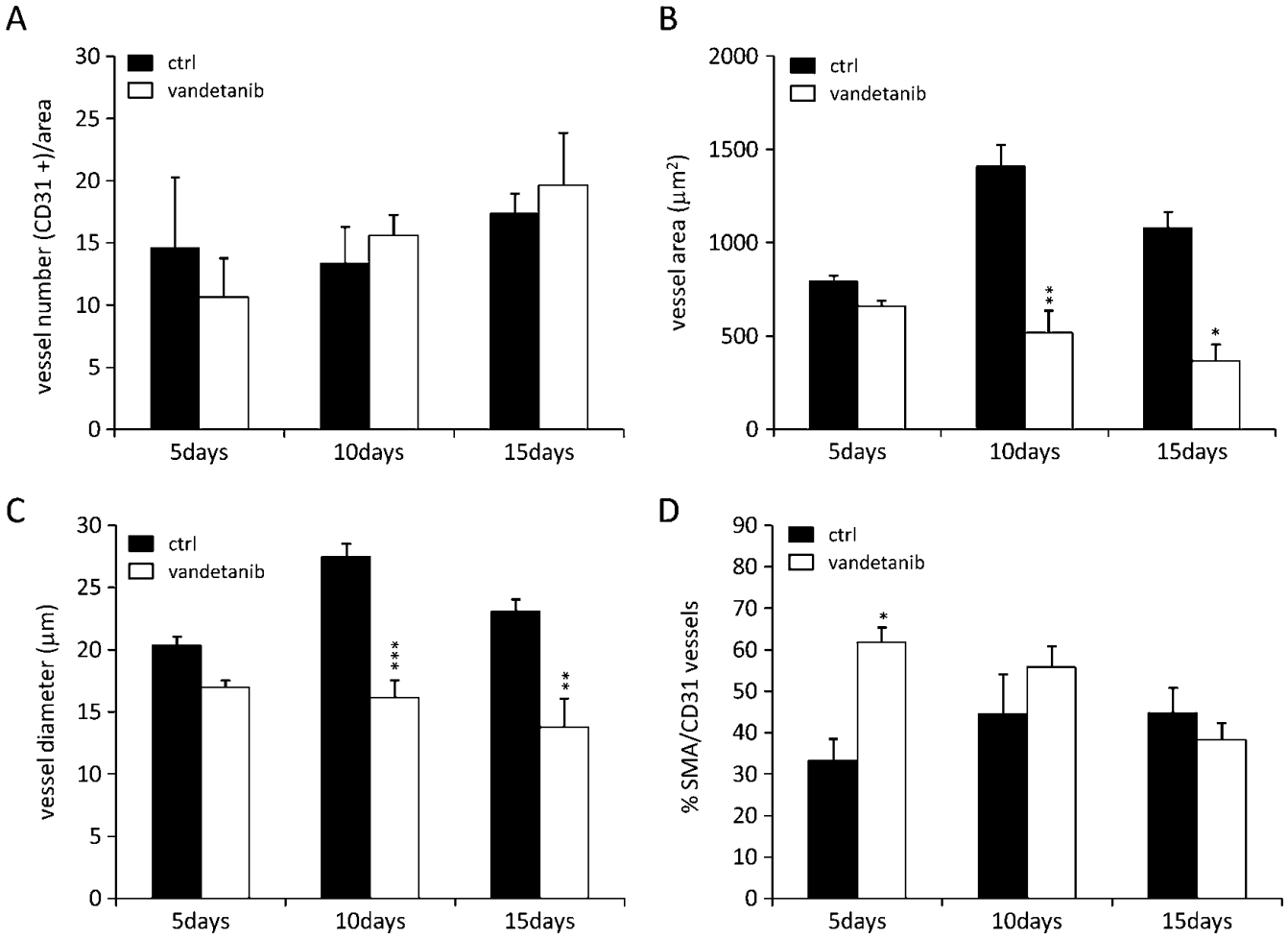


**Figure 1.** Graphical presentation of image analysis of vascular structures in A2780-1A9 xenograft tumors from mice treated for 5, 10, or 15 days with vandetanib and in time-matched controls. Vessel density (A), vessel area (B), and vessel diameter (C) were quantitatively assessed after immunostaining for CD31. Vessel maturation is given as the percentage of α-SMA/CD31 double-positive structures to all vessels (D). Bars represents mean values ± SEM ($n$ = 5 per group). *$P$ < .05, **$P$ < .01, ***$P$ < .001 *versus* controls.

Figure 3*B*, PTX tumor concentration was lower in the vandetanib-pretreated group than in the control group at 1 hour after PTX injection (starting from day 1), but at 24 hours after injection, concentrations were comparable between the two groups. To further clarify whether this result was mediated by vandetanib, we evaluated the impact of interrupting vandetanib pretreatment before PTX administration. We confirmed that after 5 days of vandetanib treatment, PTX tumor distribution was lower compared with controls 1 hour after PTX injection but comparable to controls 24 hours later (Figure 3*C.i*). In mice in which vandetanib had been suspended 5 days before PTX administration, PTX tumor distribution was comparable to controls, at each time point (Figure 3*C.ii*). However, restarting vandetanib treatment for 5 days after the 5-day interruption resulted in a reduction in PTX tumor uptake once again 1 hour after PTX injection (Figure 3*C.iii*). This indicates that the effect of vandetanib pretreatment on PTX distribution in the tumors is reversible.

### *Effect of Vandetanib on Vessel Perfusion by Hoechst 33342*

To elucidate whether the reduced tumor distribution of PTX after vandetanib pretreatment could be attributable to altered vessel perfusion, we measured perivascular Hoechst 33342 perfusion in tumors of animals treated with vandetanib for 5 or 15 days. As shown in Figures 2*C* and 4*A*, Hoechst 33342 staining around vessels was reduced in the vandetanib-treated group indicating decreased perfusion even after 5 days of vandetanib treatment (the time point at which vessel maturation index was higher than controls; Figure 1*D*). To confirm this result, an experiment was performed measuring the Hoechst 33342 content in the tumor by a quantitative HPLC assay. Tumor-bearing mice were treated with vandetanib for 5, 10, or 15 days, including a 5-day interruption (Figure 4*B*). A statistically significant decrease in Hoechst 33342 perfusion compared with the control group was observed at all time points after vandetanib pretreatment. The 5-day interruption in vandetanib treatment allowed complete recovery in vessel perfusion, with Hoechst 33342 perfusion levels comparable with untreated controls. These results are in accordance with the pharmacokinetic distribution of PTX.

### *Antitumor Activity of Vandetanib in Combination with PTX*

To study whether the timing of vandetanib pretreatment associated with modification at the tumor vasculature influenced the response to PTX treatment, tumor-bearing mice were pretreated with vandetanib for different periods (1, 5, or 10 days) before PTX. Figure 5*A* shows that all the three combination schedules were more effective than either agent alone ($T/C$ = 40%, 57%, and 68% for the groups treated

for 1, 5, and 10 days, respectively, with vandetanib plus PTX *vs* PTX alone), but no significant differences were observed among the three combinations. The antitumor effects were greater when vandetanib was administered after PTX ($T/C$ = 21% *vs* PTX alone; Figure 5*B*) compared with the reverse sequence ($T/C$ = 57% *vs* PTX alone; Figure 5*A.ii*). Mice were randomized on median tumor weight, aiming to administer PTX when tumors reached the same size as those in the vehicle-pretreated animals. To exclude the possibility that the better response in the PTX → vandetanib group might be due to the longer treatment period, the experiment was repeated, randomizing the animals on the basis of tumor weight at the beginning of treatment for both schedules. Similar results were observed with no advantage in pretreating with vandetanib (data not shown).

To study whether the reduced tumor uptake of PTX after vandetanib pretreatment affected the outcome to PTX plus vandetanib combination therapy, we treated A2780-1A9 tumor-bearing mice for 5 days with vandetanib in combination with PTX, according to two different sequences of PTX administration: PTX was administered 4 hours after the fifth dose of vandetanib (vandetanib → PTX; Figure 6*A*) or 24 hours before the first dose of vandetanib (PTX → vandetanib; Figure 6*B*). These treatment schedules were repeated for three cycles, with a 5-day break between cycles (as the pharmacokinetic studies). As shown in Figure 6 (*A* and *B*), the vandetanib plus PTX combination therapy was more effective than either agent alone. Comparing the two combination sequences, administering vandetanib after PTX (PTX → vandetanib, $T/C$ = 17% *vs* PTX alone; Figure 6*B*) seemed more effective compared with vandetanib administered before PTX (vandetanib → PTX, $T/C$ = 41% *vs* PTX alone; Figure 6*A*). Of note, the combination sequence PTX → vandetanib enhanced the tumor growth delay compared with single-agent treatment ($T - C$ = 25 days *vs* 2 and 3 days for PTX and vandetanib, respectively), whereas in the group receiving the vandetanib → PTX sequence, a slow but progressive growth was observed ($T - C$ = 13 days). In both sequences, tumors resumed their growth when treatment was suspended. Both the single-agent treatments and the combination treatment sequences were well tolerated, with no clinical signs or significant weight loss.

Because A2780-1A9 originated from an ovarian carcinoma, the activity of the combination was assessed on the growth and spread of the tumor in the peritoneal cavity [42]. Figure 6 (*C* and *D*) shows that all vehicle-treated mice developed tumors, with a median survival time of 30 days. Paclitaxel and vandetanib increased the survival of mice (ILS = 42% for PTX, ILS = 29% and 17% for vandetanib in Figure 6, *C* and *D*, respectively). With both treatment sequences the combination was more effective than either agent alone with a consistent, although not significantly different, advantage when PTX was given before vandetanib (vandetanib → PTX, ILS = 26% *vs* PTX, ILS = 39% *vs* vandetanib, ILS = 80% *vs* vehicle, Figure 6*C*;

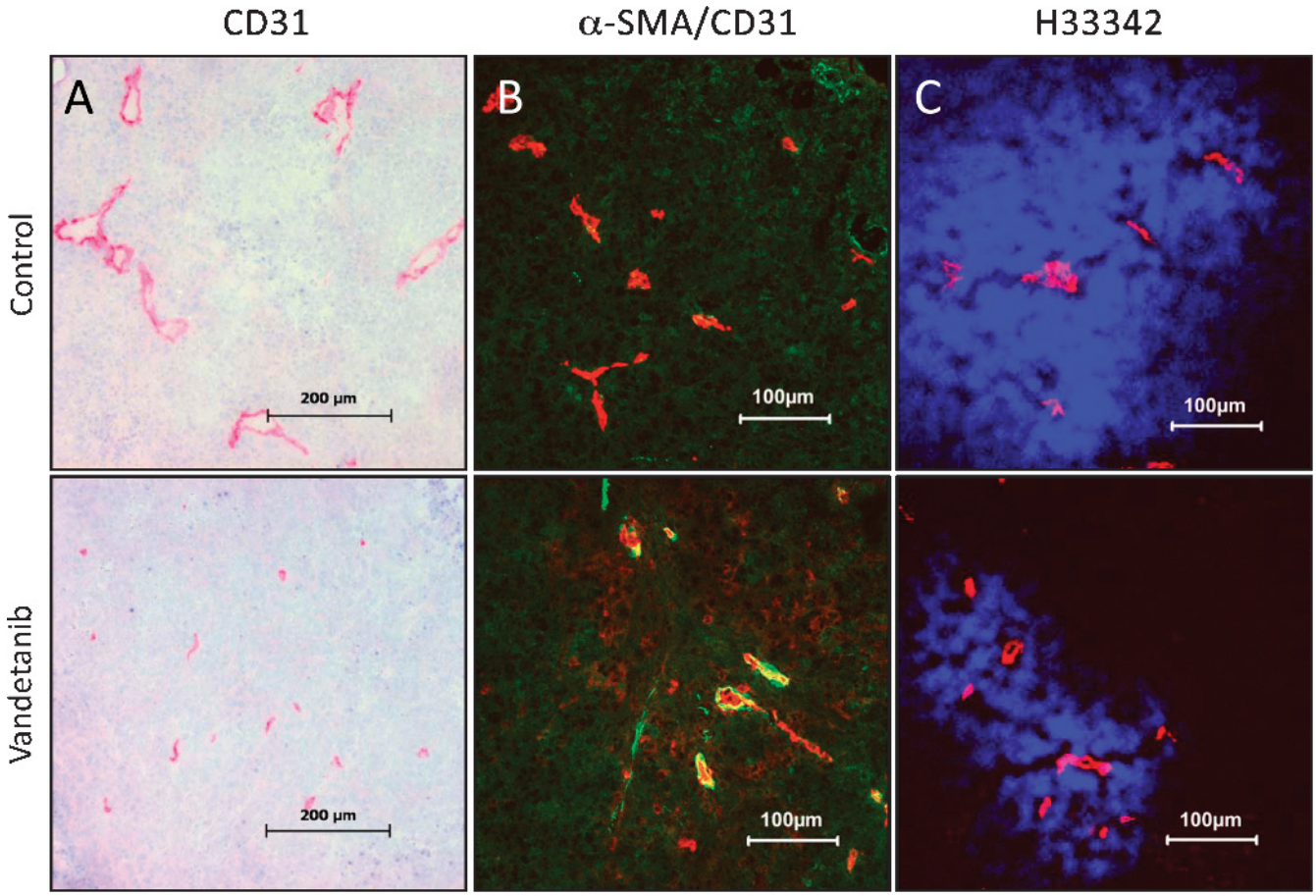


**Figure 2.** Vessel analysis on cryosections of A2780-1A9 xenograft tumors in vandetanib-treated and time-matched control animals. Representative images show differences in vessel morphology by CD31 staining (A), in vessel maturation by α-SMA (green)/CD31 (red) double-immunofluorescence staining (B), and in vessel patency by Hoechst 33342 perfusion (blue, vessels in red; C).

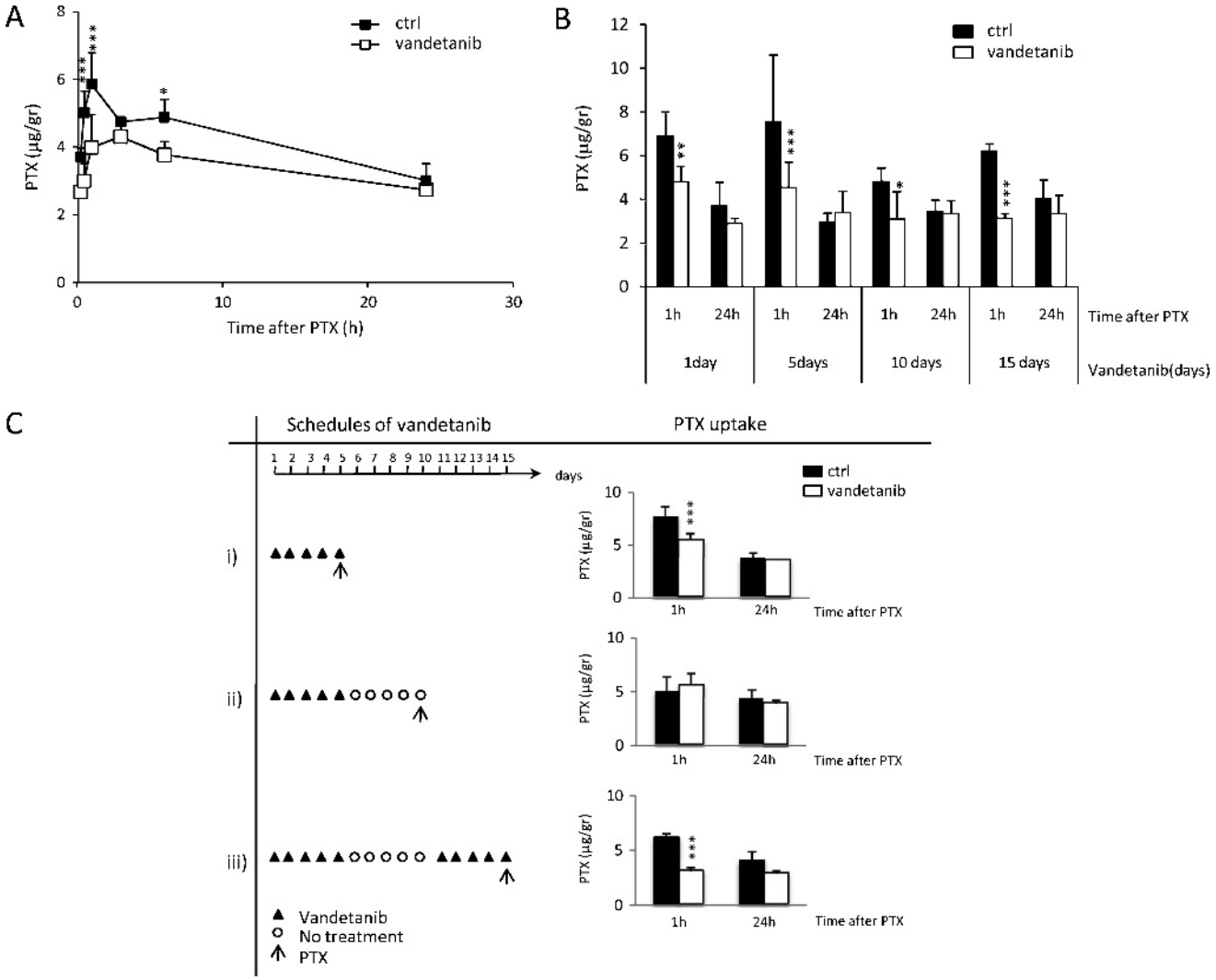


**Figure 3.** PTX distribution in A2780-1A9 xenograft tumors of vandetanib-pretreated mice. (A) PTX distribution in tumors at 15 and 30 minutes and at 1, 6, and 24 hours of mice pretreated with vandetanib or with vehicle for 5 days. (B) PTX distribution in tumors at 1 and 24 hours of mice pretreated with vandetanib or vehicle for 1, 5, 10, or 15 days. (C) PTX distribution in tumors at 1 and 24 hours following different schedules: i) vandetanib for 5 continuous days; ii) vandetanib for 5 days, an interruption of the treatment for 5 days; iii) vandetanib for 5 days, followed by a 5-day treatment interruption, and vandetanib for a further 5 days. The arrow (↑) indicate the time at which PTX was given. Values are reported as mean ± SD ($n$ = 4 per group). *$P$ < .05, **$P$ < .01, ***$P$ < .001 *versus* controls.

PTX → vandetanib, ILS = 33% *vs* PTX, ILS = 62% *vs* vandetanib, ILS = 90% *vs* vehicle, Figure 6*D*). Macroscopic analysis of the tumor burden in the peritoneal cavity of the mice at the end of treatment confirmed the decreased tumor involvement after the treatment with PTX or vandetanib as single agent (PTX more effective than vandetanib); the reduction of tumor masses in mice treated with the combinations was particularly evident, and only small tumor residuals were detected at necropsy (data not shown). This observation confirms the ability of the treatment to control tumor growth, which resumes with the suspension of the therapy.

## Discussion

Combining molecular-targeted agents with conventional chemotherapy can result in improved efficacy [7]. Vandetanib is a tyrosine kinase inhibitor of VEGFR-2, EGFR, and rearranged during transfection signaling and is being evaluated in clinical trials both as monotherapy and in combination with chemotherapy (including PTX) [39]. The present study, conducted in a xenograft tumor model in nude mice, shows the morphologic and functional changes in the tumor vasculature induced by vandetanib, the effect of vandetanib on the intratumoral delivery of PTX, and the antitumor activity of PTX. Consistent with previous observations, we have shown that the combination of vandetanib plus PTX has greater antitumor activity than single-agent treatment [36,44]. However, the changes in vascular morphology and functionality induced by vandetanib treatment were not associated with a direct increase in PTX delivery into the tumor. Rather, our results suggest that the antitumor activity of the vandetanib plus PTX combination is dependent, at least in part, on drug sequence.

Vandetanib inhibits VEGF signaling, angiogenesis and tumor growth [29]. In our model, we found that vandetanib reduced tumor vessel dimension but did not alter tumor vessel density even in responsive tumors. The relevance of vessel density as an indicator of antiangiogenic/antitumor activity has been questioned, and vessel density has not always

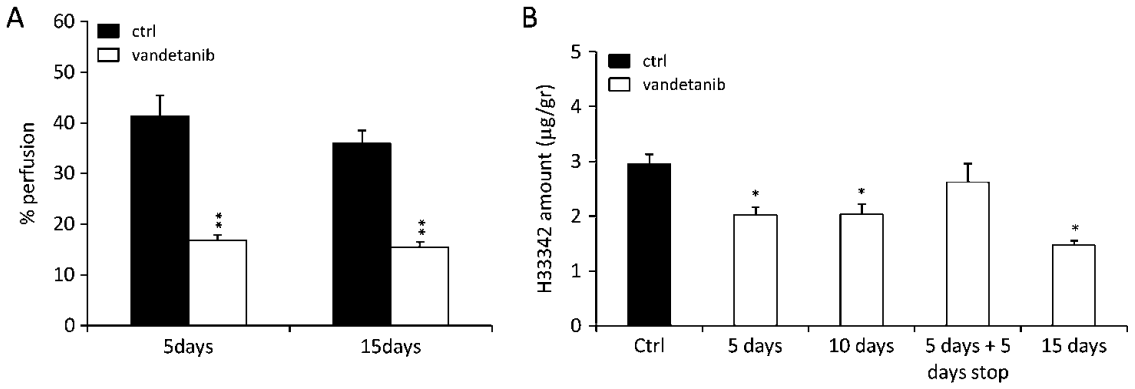


**Figure 4.** Hoechst 33342 perfusion in vandetanib-pretreated A2780-1A9 tumor-bearing mice. (A) Tumor perfusion analyzed with confocal laser scanning microscopy, after 5 and 15 days of vandetanib treatment. (B) Tumor perfusion was quantified with HPLC after 5, 10, or 15 days of vandetanib treatment and after 5 days of vandetanib treatment followed by a 5-day treatment interruption. Values are reported as mean ± SEM ($n$ = 4-5 per group). *$P$ < .05, **$P$ < .01 *versus* controls.

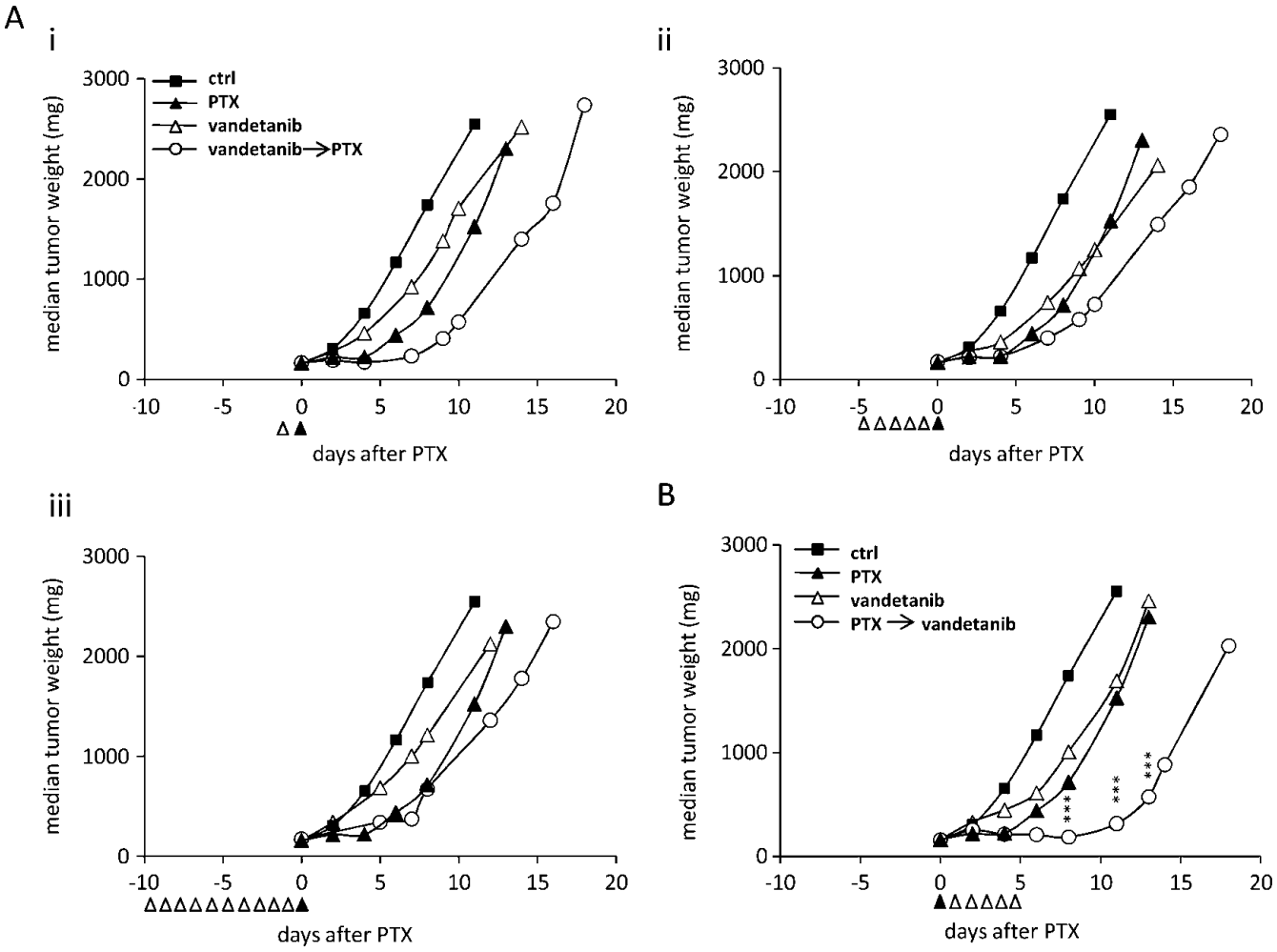


**Figure 5.** Antitumor activity of vandetanib plus PTX combination therapy on A2780-1A9 xenograft tumors. (A) Mice received vandetanib (Δ, 50 mg/kg per day), for 1 (i), 5 (ii), or 10 days (iii), and PTX (▲, 20 mg/kg) 4 hours after the last dose of vandetanib. (B) Mice received PTX (▲, 20 mg/kg) followed by vandetanib (Δ, 50 mg/kg per day for 5 days). Graphs are all from the same trial, referring to the same vehicle and PTX ($n$ = 8-10 per group). ***$P$ < .001, *versus* PTX alone.

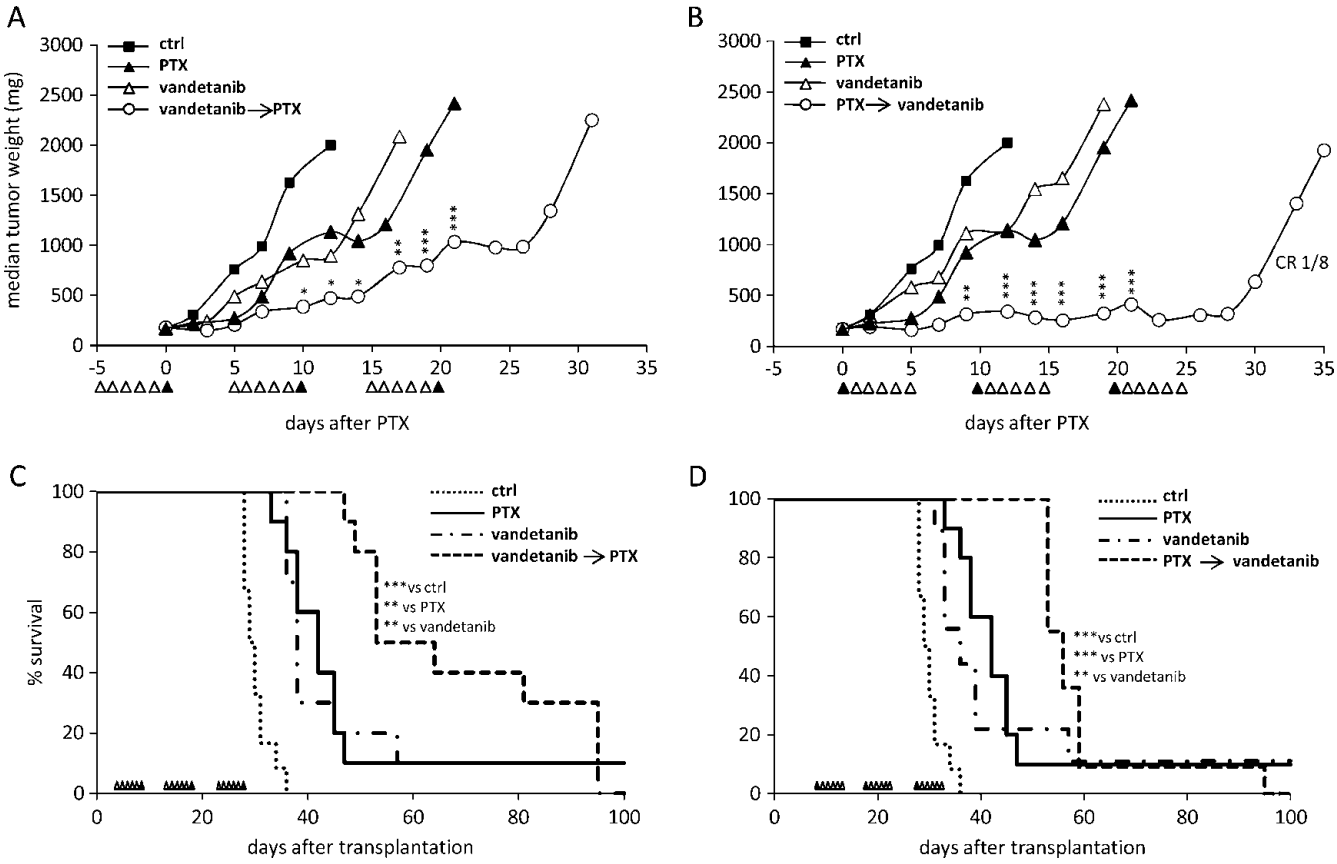


**Figure 6.** Antitumor activity of vandetanib in combination with PTX on A2780-1A9 tumor bearing mice subcutaneously (A and B) or in the peritoneal cavity (C and D). Mice received vandetanib (Δ, 50 mg/kg per day), PTX (▲, 20 mg/kg), or the combination for three cycles of 5 days. (A and C) Vandetanib → PTX: PTX was administered 4 hours after the fifth dose of vandetanib. (B and D) PTX → vandetanib: PTX was administered 24 hours before the first dose of vandetanib. Mice were randomized to start PTX treatment when median tumor weight matched in the two experimental settings (median = 150 mg, $n$ = 8-10; A and B) or at 7 days after tumor transplantation ($n$ = 10; C and D). Graphs in A and B or in C and D are from the same trial, referring to the same vehicle and PTX. *CR* indicates complete remission (mice remaining disease free for at least 4 weeks after the end of treatment). *$P < .05$, **$P < .01$, ***$P < .001$, *versus* PTX alone.

been associated with antiangiogenic efficacy [45]. Indeed, changes in the function of the tumor vascular bed might be more relevant indicators of antiangiogenic activity [46].

Jain [19] proposed that the judicious application of antiangiogenic agents may "normalize" the abnormal tumor vasculature, resulting in a more efficient delivery of drugs and oxygen to the tumor. "Normalization" has been defined as reversing the abnormalities of the vascular bed in the tumor: in the present study, vandetanib affected dilated tumor vessels, increasing the proportion of mature vessels and decreasing vessel perfusion. In addition, the term "normalization" could also be considered as an overall increase in the delivery of chemotherapy during the "normalization window" [20–23]. However, in our model, we observed decreased PTX delivery after vandetanib treatment at early time points (1 hour after PTX) compared with control, although similar tumor PTX levels were present in the vandetanib-pretreated and the control animals at a later time point (i.e., 24 hours after PTX). As plasma data exclude reduced drug availability, we hypothesize that this could possibly be because PTX penetration on tumor was less efficient because of the poorer perfusion in vandetanib-treated animals. The association between vandetanib treatment and reduced tumor delivery of PTX was further demonstrated by the observation that stopping vandetanib treatment restored PTX uptake by tumor tissue to levels similar to the matched controls and, moreover, that restarting vandetanib treatment resulted in a reduction of PTX distribution to the tumor once again.

Increased delivery of chemotherapy after antiangiogenic therapy is not a general finding. For example, although several preclinical studies have shown increased intratumoral drug uptake, after VEGF/VEGFR antibody treatment (e.g., bevacizumab) [20,22,23], decreased drug uptake has been observed with other inhibitors of angiogenesis, including RTKIs (for review, see [28]). We believe that our findings are not likely to be specific for PTX but rather reflect a decrease in

**Table 1.** Main Pharmacokinetic Parameters of PTX Distribution in Plasma and Tumor Tissues of Vandetanib Pretreated Mice.

| Tissue | Treatment | $C_{max}$ (μg/g; μg/ml) | $T_{max}$ (h) | AUC (μg/g; μg/ml) | $T_{1/2}$ (h) |
|---|---|---|---|---|---|
| Tumor | Control | 5.9 | 1.00 | 100.6 | 29.80 |
| | Vandetanib | 4.3 | 3.00 | 82.0 | 34.50 |
| Plasma | Control | 30.1 | 0.17 | 26.1 | 0.52 |
| | Vandetanib | 31.8 | 0.17 | 33.0 | 0.63 |

Experiment was performed as in Figure 3*A*.
*AUC* indicates area under the concentration *versus* time curve; $C_{max}$, maximal drug concentration; $T_{max}$, time at which the $C_{max}$ was found; $T_{1/2}$, terminal elimination half-life.

tumor perfusion because Hoechst 33342 level, indicators of vascular perfusion [47], was reduced in the tumors of mice pretreated with vandetanib. A more detailed analysis of vessel and drug distribution would be needed to determine the degree of heterogeneity that might be hidden within an overall decreased perfusion over the whole tumor [48]. For example, better-perfused vessels that remain after vandetanib may allow increased delivery of PTX in certain regions of the tumor.

However, even if tumor vessels were "normalized" by vandetanib in the current study, there seemed to be neither a clear efficacy advantage in pretreating with vandetanib before PTX nor a dependence from the length of vandetanib pretreatment (Figure 5), the best antitumor response being observed with the schedule of PTX administered before vandetanib. This suggests that the overall therapeutic response to RTKI plus chemotherapy combinations might be improved by appropriate sequencing of the individual agents.

The scheduling of combination regimens that include a small-molecule RTKI is often guided by *in vitro* studies. In the case of vandetanib, differences in outcome of the *in vitro* and *in vivo* sequencing studies may be due to context-dependent effects of EGFR and VEGFR inhibition in the different assay systems. EGFR-dependent effects of vandetanib are likely to dominate in *in vitro* assays where there is no role for VEGF-dependent new angiogenesis, whereas VEGFR-2–dependent antiangiogenic effects of vandetanib may dominate *in vivo* [35,44]. It is unlikely that the effects of vandetanib observed in this study were mediated by effects on EGFR signaling because A2780-1A9 cells did not respond, either *in vitro* or *in vivo*, to gefitinib, a highly selective EGFR inhibitor (data not shown).

We used a schedule of 5 days of vandetanib treatment to allow vandetanib to exert its effects on the tumor vasculature, followed by a 5-day interruption in therapy to allow recovery of the vascular bed and improved PTX distribution into the tumor. The different response of the two sequences might reflect the distribution of PTX in the tumor as previously discussed, although the tumor level of PTX at 24 hours after its administration was comparable to controls. The different response to the combination therapy is not influenced by the size of the tumor at the beginning of the treatment with PTX (same weight in the two schedules; Figure 6) or by the duration of the treatment (same duration; data not shown). In fact, tumors seemed to respond as long as the animals were treated, but when treatment stopped, tumor growth resumed at a rate similar to untreated controls. Further understanding of the therapeutic interaction between chemotherapy (i.e., PTX) and RTKI (i.e., vandetanib) may provide important explanations of the overall tumor response.

Also, in the orthotopic model of tumor spreading in the peritoneal cavity, the combination of the two agents was able to control the tumor growth only for the duration of the treatment (as confirmed by necropsy of the mice at the end of treatment). In this setting, a clear advantage with either one of the two sequences was not observed. We recognize that there are limitations to this model. We have focused on tumor masses spreading into the peritoneal sites, where angiogenesis might not be predominant for their initial growth and PTX distribution might not be influenced by modification of the vasculature. Further studies on more complex models are necessary to assess the relevance of these findings in ovarian carcinoma [49]. Nevertheless, the results of this study have potentially important implications for the design of trials with agents that target multiple growth factor pathways in combination with chemotherapy. They indicate that the sequence of the drugs may be crucial in optimizing tumor response during combination schedules. Robust tumor pharmacodynamics and pharmacokinetics could assist the fine-tuning of drug timing and sequences and might ultimately improve antitumor activity.

## Acknowledgments

The authors thank Gillian Hill, freelance writer, who provided editing assistance as funded by AstraZeneca. Zactima™ is a registered trademark of the AstraZeneca group of companies.

## References

[1] Folkman J (2003). Fundamental concepts of the angiogenic process. *Curr Mol Med* **3**, 643–651.

[2] Folkman J (2007). Angiogenesis: an organizing principle for drug discovery? *Nat Rev Drug Discov* **6**, 273–286.

[3] Yu JL, Coomber BL, and Kerbel RS (2002). A paradigm for therapy-induced microenvironmental changes in solid tumors leading to drug resistance. *Differentiation* **70**, 599–609.

[4] El Emir E, Qureshi U, Dearling JL, Boxer GM, Clatworthy I, Folarin AA, Robson MP, Nagl S, Konerding MA, and Pedley RB (2007). Predicting response to radioimmunotherapy from the tumor microenvironment of colorectal carcinomas. *Cancer Res* **67**, 11896–11905.

[5] Taraboletti G and Margosio B (2001). Antiangiogenic and antivascular therapy for cancer. *Curr Opin Pharmacol* **1**, 378–384.

[6] Ferrara N and Kerbel RS (2005). Angiogenesis as a therapeutic target. *Nature* **438**, 967–974.

[7] Gasparini G, Longo R, Fanelli M, and Teicher BA (2005). Combination of antiangiogenic therapy with other anticancer therapies: results, challenges, and open questions. *J Clin Oncol* **23**, 1295–1311.

[8] Volk LD, Flister MJ, Bivens CM, Stutzman A, Desai N, Trieu V, and Ran S (2008). Nab-paclitaxel efficacy in the orthotopic model of human breast cancer is significantly enhanced by concurrent anti–vascular endothelial growth factor A therapy. *Neoplasia* **10**, 613–623.

[9] Ferrara N, Hillan KJ, Gerber HP, and Novotny W (2004). Discovery and development of bevacizumab, an anti-VEGF antibody for treating cancer. *Nat Rev Drug Discov* **3**, 391–400.

[10] Hurwitz H, Fehrenbacher L, Novotny W, Cartwright T, Hainsworth J, Heim W, Berlin J, Baron A, Griffing S, Holmgren E, et al. (2004). Bevacizumab plus irinotecan, fluorouracil, and leucovorin for metastatic colorectal cancer. *N Engl J Med* **350**, 2335–2342.

[11] Giavazzi R, Bani MR, and Taraboletti G (2007). Tumor-host interaction in the optimization of paclitaxel-based combination therapies with vascular targeting compounds. *Cancer Metastasis Rev* **26**, 481–488.

[12] Teicher BA (1996). A systems approach to cancer therapy. (Antioncogenics + standard cytotoxics → mechanism(s) of interaction). *Cancer Metastasis Rev* **15**, 247–272.

[13] Minchinton AI and Tannock IF (2006). Drug penetration in solid tumours. *Nat Rev Cancer* **6**, 583–592.

[14] McDonald DM and Choyke PL (2003). Imaging of angiogenesis: from microscope to clinic. *Nat Med* **9**, 713–725.

[15] Thorpe PE (2004). Vascular targeting agents as cancer therapeutics. *Clin Cancer Res* **10**, 415–427.

[16] Baluk P, Hashizume H, and McDonald DM (2005). Cellular abnormalities of blood vessels as targets in cancer. *Curr Opin Genet Dev* **15**, 102–111.

[17] Jain RK (2001). Normalizing tumor vasculature with anti-angiogenic therapy: a new paradigm for combination therapy. *Nat Med* **7**, 987–989.

[18] Hagendoorn J, Tong R, Fukumura D, Lin Q, Lobo J, Padera TP, Xu L, Kucherlapati R, and Jain RK (2006). Onset of abnormal blood and lymphatic vessel function and interstitial hypertension in early stages of carcinogenesis. *Cancer Res* **66**, 3360–3364.

[19] Jain RK (2005). Normalization of tumor vasculature: an emerging concept in antiangiogenic therapy. *Science* **307**, 58–62.

[20] Wildiers H, Guetens G, De Boeck G, Verbeken E, Landuyt B, Landuyt W, de Bruijn EA, and van Oosterom AT (2003). Effect of antivascular endothelial growth factor treatment on the intratumoral uptake of CPT-11. *Br J Cancer* **88**, 1979–1986.

[21] Winkler F, Kozin SV, Tong RT, Chae SS, Booth MF, Garkavtsev I, Xu L, Hicklin DJ, Fukumura D, di Tomaso E, et al. (2004). Kinetics of vascular normalization by VEGFR2 blockade governs brain tumor response to radiation: role of oxygenation, angiopoietin-1, and matrix metalloproteinases. *Cancer Cell* **6**, 553–563.

[22] Tong RT, Boucher Y, Kozin SV, Winkler F, Hicklin DJ, and Jain RK (2004). Vascular normalization by vascular endothelial growth factor receptor 2 blockade induces a pressure gradient across the vasculature and improves drug penetration in tumors. *Cancer Res* **64**, 3731–3736.

[23] Dickson PV, Hamner JB, Sims TL, Fraga CH, Ng CY, Rajasekeran S, Hagedorn NL, McCarville MB, Stewart CF, and Davidoff AM (2007). Bevacizumab-induced transient remodeling of the vasculature in neuroblastoma xenografts results in improved delivery and efficacy of systemically administered chemotherapy. *Clin Cancer Res* **13**, 3942–3950.

[24] Franco M, Man S, Chen L, Emmenegger U, Shaked Y, Cheung AM, Brown AS, Hicklin DJ, Foster FS, and Kerbel RS (2006). Targeted anti–vascular endothelial growth factor receptor-2 therapy leads to short-term and long-term impairment of vascular function and increase in tumor hypoxia. *Cancer Res* **66**, 3639–3648.

[25] Ellis LM and Hicklin DJ (2008). VEGF-targeted therapy: mechanisms of anti-tumour activity. *Nat Rev Cancer* **8**, 579–591.

[26] Smith JK, Mamoon NM, and Duhe RJ (2004). Emerging roles of targeted small molecule protein-tyrosine kinase inhibitors in cancer therapy. *Oncol Res* **14**, 175–225.

[27] Karaman MW, Herrgard S, Treiber DK, Gallant P, Atteridge CE, Campbell BT, Chan KW, Ciceri P, Davis MI, Edeen PT, et al. (2008). A quantitative analysis of kinase inhibitor selectivity. *Nat Biotechnol* **26**, 127–132.

[28] Ma J and Waxman DJ (2008). Combination of antiangiogenesis with chemotherapy for more effective cancer treatment. *Mol Cancer Ther* **7**, 3670–3684.

[29] Wedge SR, Ogilvie DJ, Dukes M, Kendrew J, Chester R, Jackson JA, Boffey SJ, Valentine PJ, Curwen JO, Musgrove HL, et al. (2002). ZD6474 inhibits vascular endothelial growth factor signaling, angiogenesis, and tumor growth following oral administration. *Cancer Res* **62**, 4645–4655.

[30] Ciardiello F, Caputo R, Damiano V, Troiani T, Vitagliano D, Carlomagno F, Veneziani BM, Fontanini G, Bianco AR, and Tortora G (2003). Antitumor effects of ZD6474, a small molecule vascular endothelial growth factor receptor tyrosine kinase inhibitor, with additional activity against epidermal growth factor receptor tyrosine kinase. *Clin Cancer Res* **9**, 1546–1556.

[31] Wu W, Onn A, Isobe T, Itasaka S, Langley RR, Shitani T, Shibuya K, Komaki R, Ryan AJ, Fidler IJ, et al. (2007). Targeted therapy of orthotopic human lung cancer by combined vascular endothelial growth factor and epidermal growth factor receptor signaling blockade. *Mol Cancer Ther* **6**, 471–483.

[32] Yano S, Muguruma H, Matsumori Y, Goto H, Nakataki E, Edakuni N, Tomimoto H, Kakiuchi S, Yamamoto A, Uehara H, et al. (2005). Antitumor vascular strategy for controlling experimental metastatic spread of human small-cell lung cancer cells with ZD6474 in natural killer cell–depleted severe combined immunodeficient mice. *Clin Cancer Res* **11**, 8789–8798.

[33] Beaudry P, Nilsson M, Rioth M, Prox D, Poon D, Xu L, Zweidler-Mckay P, Ryan A, Folkman J, Ryeom S, et al. (2008). Potent antitumor effects of ZD6474 on neuroblastoma via dual targeting of tumor cells and tumor endothelium. *Mol Cancer Ther* **7**, 418–424.

[34] Williams KJ, Telfer BA, Brave S, Kendrew J, Whittaker L, Stratford IJ, and Wedge SR (2004). ZD6474, a potent inhibitor of vascular endothelial growth factor signaling, combined with radiotherapy: schedule-dependent enhancement of antitumor activity. *Clin Cancer Res* **10**, 8587–8593.

[35] Troiani T, Lockerbie O, Morrow M, Ciardiello F, and Eckhardt SG (2006). Sequence-dependent inhibition of human colon cancer cell growth and of pro-survival pathways by oxaliplatin in combination with ZD6474 (Zactima), an inhibitor of VEGFR and EGFR tyrosine kinases. *Mol Cancer Ther* **5**, 1883–1894.

[36] Bianco C, Giovannetti E, Ciardiello F, Mey V, Nannizzi S, Tortora G, Troiani T, Pasqualetti F, Eckhardt G, de Liguoro M, et al. (2006). Synergistic antitumor activity of ZD6474, an inhibitor of vascular endothelial growth factor receptor and epidermal growth factor receptor signaling, with gemcitabine and ionizing radiation against pancreatic cancer. *Clin Cancer Res* **12**, 7099–7107.

[37] Gustafson DL, Frederick B, Merz AL, and Raben D (2008). Dose scheduling of the dual VEGFR and EGFR tyrosine kinase inhibitor vandetanib (ZD6474, Zactima) in combination with radiotherapy in EGFR-positive and EGFR-null human head and neck tumor xenografts. *Cancer Chemother Pharmacol* **61**, 179–188.

[38] Herbst RS, Heymach JV, O'Reilly MS, Onn A, and Ryan AJ (2007). Vandetanib (ZD6474): an orally available receptor tyrosine kinase inhibitor that selectively targets pathways critical for tumor growth and angiogenesis. *Expert Opin Investig Drugs* **16**, 239–249.

[39] Heymach JV, Paz-Ares L, De Braud F, Sebastian M, Stewart DJ, Eberhardt WE, Ranade AA, Cohen G, Trigo JM, Sandler AB, et al. (2008). Randomized phase II study of vandetanib alone or with paclitaxel and carboplatin as first-line treatment for advanced non–small-cell lung cancer. *J Clin Oncol* **26**, 5407–5415.

[40] Markman M (2008). Pharmaceutical management of ovarian cancer: current status. *Drugs* **68**, 771–789.

[41] Bani MR, Nicoletti MI, Alkharouf NW, Ghilardi C, Petersen D, Erba E, Sausville EA, Liu ET, and Giavazzi R (2004). Gene expression correlating with response to paclitaxel in ovarian carcinoma xenografts. *Mol Cancer Ther* **3**, 111–121.

[42] Manenti L, Riccardi E, Marchini S, Naumova E, Floriani I, Garofalo A, Dossi R, Marrazzo E, Ribatti D, Scanziani E, et al. (2005). Circulating plasma vascular endothelial growth factor in mice bearing human ovarian carcinoma xenograft correlates with tumor progression and response to therapy. *Mol Cancer Ther* **4**, 715–725.

[43] Naumova E, Ubezio P, Garofalo A, Borsotti P, Cassis L, Riccardi E, Scanziani E, Eccles SA, Bani MR, and Giavazzi R (2006). The vascular targeting property of paclitaxel is enhanced by SU6668, a receptor tyrosine kinase inhibitor, causing apoptosis of endothelial cells and inhibition of angiogenesis. *Clin Cancer Res* **12**, 1839–1849.

[44] Troiani T, Serkova NJ, Gustafson DL, Henthorn TK, Lockerbie O, Merz A, Long M, Morrow M, Ciardiello F, and Eckhardt SG (2007). Investigation of two dosing schedules of vandetanib (ZD6474), an inhibitor of vascular endothelial growth factor receptor and epidermal growth factor receptor signaling, in combination with irinotecan in a human colon cancer xenograft model. *Clin Cancer Res* **13**, 6450–6458.

[45] Hlatky L, Hahnfeldt P, and Folkman J (2002). Clinical application of anti-angiogenic therapy: microvessel density, what it does and doesn't tell us. *J Natl Cancer Inst* **94**, 883–893.

[46] Hicklin DJ (2007). Promoting angiogenesis to a fault. *Nat Biotechnol* **25**, 300–302.

[47] Smith KA, Hill SA, Begg AC, and Denekamp J (1988). Validation of the fluorescent dye Hoechst 33342 as a vascular space marker in tumours. *Br J Cancer* **57**, 247–253.

[48] Czabanka M, Vinci M, Heppner F, Ullrich A, and Vajkoczy P (2009). Effects of sunitinib on tumor hemodynamics and delivery of chemotherapy. *Int J Cancer* **124**, 1293–1300.

[49] Lu C, Thaker PH, Lin YG, Spannuth W, Landen CN, Merritt WM, Jennings NB, Langley RR, Gershenson DM, Yancopoulos GD, et al. (2008). Impact of vessel maturation on antiangiogenic therapy in ovarian cancer. *Am J Obstet Gynecol* **198**, 477.e471–477.e479; discussion 477.e479–477.e410.

## Supplementary Data

### *Supplementary Information 1*

*Immunopathologic analyses.* Cryosections (4 μm) were fixed for 1 minute in methanol and for 8 minutes in acetone at room temperature and processed as follows.

*Vessel density and morphology.* Vessel density and morphology were assessed by immunostaining with anti-CD31 antibody MEC13.3 (Beckton Dickinson GmbH, Heidelberg, Germany), a biotin-conjugated mouse anti–rat immunoglobulin G subclass 1/2a monoclonal antibody (clone G28-5; Beckton Dickinson GmbH), and the streptavidin-AP reagent/chromogen of the Dako REAL Detection System AP/RED (Dako Deutschland GmbH, Hamburg, Germany). Three randomly selected measurement fields (0.94 $mm^2$) from each tumor with the highest vessel density (hot spots) were scanned, and all CD31-stained vessel structures were marked by the examiner. The vessel density, vessel area, and vessel diameter (represented by the shortest Feret's diameter) were determined using computer aided image analysis software (AxioVision Rel. 4.6.2; Zeiss, Oberkochen, Germany).

*Vessel maturation index.* Vessel maturation was assessed by quantification of blood vessels showing colocalization of α-SMA and CD31-positive cells. Sections were stained with anti-CD31 antibody MEC13.3 visualized with a Cy3-conjugated goat anti-rat immunoglobulin G/immunoglobulin M serum (Dianova, Hamburg, Germany) followed by incubation with a biotinylated anti–α-SMA antibody (clone 1A4; Dako Deutschland GmbH). Biotinylation was performed using the Animal Research Kit (Dako Deutschland GmbH) following the manufacturer's instructions. Biotinylated antibodies were detected with fluorescein isothiocyanate–conjugated streptavidin (Dako Deutschland GmbH). Double immunofluorescence was analyzed by confocal laser scanning microscopy (cLSM; LSM510, Zeiss) as recently described [1]. From each tumor, five randomly selected measurement fields of 0.2 $mm^2$ were scanned, and all CD31-stained vessels and all CD31/α-SMA double-positive vessels were counted. Vessel maturation index was represented as α-SMA–positive vessels as a percentage of total CD31-positive vessels.

*Vessel perfusion.* Sections of Hoechst 33342 perfused tumors were CD31 stained for immunofluorescence microscopy as previously described. Immediately after immunostaining, sections were analyzed with the cLSM. Four randomly selected vascularized areas of each tumor (detection area, 0.21 $mm^2$) were scanned: for CD31 fluorescence scanning the HeNe (543 nm) laser was combined with the light filter LP 560 (Zeiss). The Hoechst 33342 fluorochrome was excited using an HBO mercury lamp (OSRAM GmbH, Berlin, Germany), and the emitted fluorescence light was detected.

A detection level for blue pixels (Hoechst fluorescence intensity) was defined using tumors with low and highly patent vessels. The pixel number and pixel area were automatically calculated in all images using the colocalization analysis software tool of cLSM. Subsequently, the blue pixel area was set in percent of the whole scanned area. The mean value and SEM of the blue pixel area were calculated using the images of all animals per group.

To confirm the cLSM result, Hoechst 33342 levels in tumors were also quantified by HPLC analysis. Briefly, tumor samples were homogenized in $CH_3CN$ (1:2 wt/vol) and 0.2 ml of the homogenate added with 20 μl of SN38 (2 μM) as internal standard. Samples were centrifuged at 13,000 rpm for 10 minutes, and 150 μl of the organic phase was added with 150 μl of 0.2 M ammonium acetate buffer pH 5 and injected in the HPLC. Chromatographic separation was carried out on Symmetry Shield RP18 (3.5 μm, 4.6 × 150 mm) column (Waters, Millford, MA) and gradient elution from 0.1 M $CH_3COOH$ pH 5/$CH_3CN$/$CH_3OH$ 80:10:10 to 35:20:45 during a 20-minute period. The flow rate was of 1 ml/min. Fluorimetric detection was performed at $\lambda_{ex}$ = 376 nm and $\lambda_{em}$ = 534 nm.

### *Supplementary Information 2*

*Pharmacokinetic analysis*

*Plasma PTX assays.* Plasma samples (0.3 ml) were spiked with 1 μg of docetaxel (Indena S.p.A.) as internal standard and 200 μl of 0.2 M ammonium acetate buffer pH 5 was added. After centrifugation, supernatants were processed using a Rapid Trace SPE workstation (Zymark, Hopkinton, MA), with Sep-Pak CN cartridge for solid-phase extraction (Waters). PTX was eluted from the columns with 1 ml of 0.1% triethylamine in $CH_3CN$. The eluents were dried under nitrogen, and the residues were reconstituted in 120 μl of mobile phase and injected into the HPLC system. Chromatographic separation was carried out on Novo Pak C18 (3.9 × 150 mm) column (Waters) and isocratic mobile phase of 0.01 M $CH_3COONH_4$ pH 5/$CH_3CN$/$CH_3OH$/THF 59:34:6:1 with a flow rate 1.3 ml/min. UV detection was performed at 230 nm (2462 Dual λ Absorbance Detector; Waters). Control mouse plasma was used to prepare a calibration curve over the range 0.33 to 16.7 μg/ml of PTX.

*Tumor PTX assays.* Tumor samples were homogenized in 0.2 M $CH_3COONH_4$ pH 5 (1:4 wt/vol), and 1 ml of homogenate sample was added with 1 μg of IDN5390 (Indena S.p.A.) as internal standard and extracted with 5 ml of $CH_3CN$. Samples were centrifuged at 4000 rpm for 10 minutes. The organic phase was separated and dried under nitrogen, and the residues were dissolved with 120 μl of mobile phase and 30 μl of SSA 1% (wt/vol). One hundred microliters of the reconstitute samples was injected in the HPLC and analyzed with a Symmetry C18 (3.5 μm, 4.6 × 150 mm) column (Waters) using a mobile phase of $CH_3CN$/0.01 M $CH_3COONH_4$ pH 5/$CH_3OH$ 39:51:10, a flow rate of 1.3 ml/min, and UV detection at 230 nm. Tissues obtained from control mice were used to prepare the calibration curve by the addition of PTX.

## Reference

[1] Franz M, Hansen T, Borsi L, Geier C, Hyckel P, Schleier P, Richter P, Altendorf-Hofmann A, Kosmehl H, and Brendt A (2007). A quantitative co-localization analysis of large unspliced tenascin-C(L) and laminin-5/gamma2-chain in basement membranes of oral squamous cell carcinoma by confocal laser scanning microscopy. *J Oral Pathol Med* **36**, 6–11.